Chemistry–A European Journal
Research Article
doi.org/10.1002/chem.202202507
Chemistry Europe
European Chemical Societies Publishing
www.chemeurj.org

Thiazole Boron Difluoride Dyes with Large Stokes Shift, Solid State Emission and Room-Temperature Phosphorescence

Wei Wang,[a, d] Shuo Tong,*[b] Qi-Qiang Wang,[a, d] Yu-Fei Ao,[a, d] De-Xian Wang,*[a, d] and Jieping Zhu*[c]

Abstract: The small Stokes shift and weak emission in the solid state are two main shortcomings associated with the boron-dipyrromethene (BODIPY) family of dyes. This study presents the design, synthesis and luminescent properties of boron difluoro complexes of 2-aryl-5-alkylamino-4-alkylaminocarbonylthiazoles. These dyes display Stokes shifts ($\Delta\lambda$, 77–101 nm) with quantum yields (ϕ_{FL}) up to 64.9 and 34.7% in toluene solution and in solid state, respectively. Some of these compounds exhibit dual fluorescence and room-temperature phosphorescence (RTP) emission properties with modulable phosphorescence quantum yields (ϕ_{PL}) and lifetime (τ_p up to 251 μs). The presence of intramolecular H-bonds and negligible π-π stacking revealed by X-ray crystal structure might account for the observed large Stokes shift and significant solid-state emission of these fluorophores, while the enhanced spin-orbit coupling (SOC) of iodine and the self-assembly driven by halogen bonding, π-π and C–H···π interactions could be responsible for the observed RTP of iodine containing phosphors.

Introduction

Boron-dipyrromethenes (BODIPYs) have received intensive attentions owing to their fascinating photophysical properties (Scheme 1a).[1,2] Their narrow absorption and emission bands in

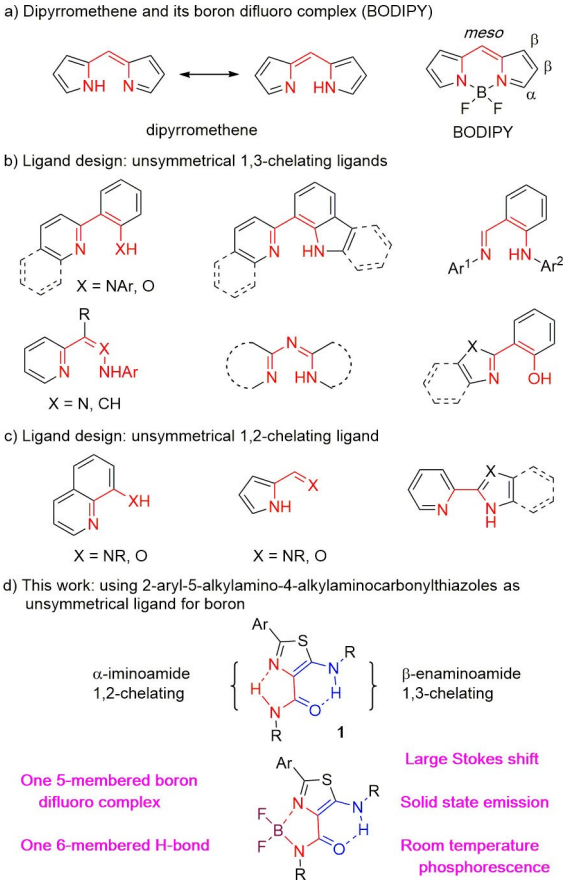

Scheme 1. BODIPY and its analogues: Breaking symmetry for better photophysical properties.

[a] W. Wang, Prof. Dr. Q.-Q. Wang, Prof. Dr. Y.-F. Ao, Prof. Dr. D.-X. Wang
Beijing National Laboratory for Molecular Sciences
CAS Key Laboratory of Molecular Recognition and Function
Institute of Chemistry
Chinese Academy of Sciences, Beijing 100190 (P. R. China)
E-mail: dxwang@iccas.ac.cn
Homepage: http://dxwang.iccas.ac.cn/

[b] Prof. Dr. S. Tong
MOE Key Laboratory of Bioorganic Phosphorus Chemistry and Chemical Biology
Department of Chemistry
Tsinghua University, Beijing 100084 (P. R. China)
E-mail: tongshuo@mail.tsinghua.edu.cn
Homepage: https://mascl.group

[c] Prof. Dr. J. Zhu
Laboratory of Synthesis and Natural Products (LSPN)
Institute of Chemical Sciences and Engineering
Ecole Polytechnique Fédérale de Lausanne, EPFL-SB-ISIC-LSPN, BCH5304
1015 Lausanne (Switzerland)
E-mail: jieping.zhu@epfl.ch
Homepage: https://www.epfl.ch/labs/lspn/

[d] W. Wang, Prof. Dr. Q.-Q. Wang, Prof. Dr. Y.-F. Ao, Prof. Dr. D.-X. Wang
University of Chinese Academy of Sciences
Beijing 100049 (P. R. China)

Supporting information for this article is available on the WWW under https://doi.org/10.1002/chem.202202507

visible spectral region, high molar absorption coefficients and high fluorescence quantum yields in conjunction with their excellent thermal and photochemical stabilities have made them attractive fluorescent dyes for applications in, for instance, bioimaging/detection, photodynamic therapy (PDT),[3,4] photovoltaic devices,[5] solar cells,[6] and fluorescent indicators,[7] etc. The small Stokes shift due to the *pseudo* C_2-symmetry of the BODIPYs and consequently, weak emission in the solid state have nevertheless limited their applicability in biological systems and materials science. To address these drawbacks, the impact of peripheral decoration of BODIPY core at α-, β- and *meso*-positions on its fluorescence properties has been extensively examined.[1,7,8] Alternatively, boron complexes using unsymmetrical ligands to differentiate energetically the ground and the excited states have also been investigated.[2] Towards this end, both N^N and N^O bidentate molecules using aniline, indole, isoindolin-1-one, carbazole, phenol as anionic N-donor and pyridine, quinoline, pyrimidine, thiazole, imine, hydrazone, sp^2 carbon as imino N-donor equivalents have been examined. This strategy turned out to be rewarding as a number of boron complexes with improved photophysical properties have been developed.[2,9–31] From viewpoint of structural design, most of these ligands contain formally a β-enaminoimine and to a less extent, a 3-iminoprop-1-enol motif which, upon reaction with BF_3 etherate, would produce a 6-membered boron complex as it is found in BODIPY (Scheme 1b). Interestingly, boron difluoro complexes of 1,2-chelating ligands have been less investigated as fluorophores (Scheme 1c),[28] although their transition metal complexes have been extensively used in dye-sensitized solar cells and as photoredox catalysts in organic synthesis.

In stark contrast with the extensive efforts dedicated to improve the fluorescence (FL) properties of BODIPY, research on phosphorescence of BODIPY remains relatively rare.[32,33] The inefficient intersystem crossing (ISC) of the excited singlet state to the triplet-state and the conformational flexibility of small organic molecules in general could indeed limit their applications as phosphorescent dyes. Besides exploiting the heavy atom effect to facilitate the ISC process, several approaches including supramolecular interactions, co-polymerization and crystal engineering[34,35] have been developed to physically constrain the molecular motion, reducing consequently the non-radiative decay of the electron in the triplet state. Notwithstanding the successful examples, amorphous metal-free organic molecules displaying room-temperature phosphorescence (RTP) remain rare although they have advantages over inorganic phosphors and transition metal complexes such as cost efficiency, lower toxicity and structural tunability.[36,37]

We have recently reported the synthesis and luminescent properties of 5-amino-4-aminocarbonylthiazoles **1**.[38] Structurally, two intramolecular hydrogen bonds lock the thiazole **1** into a *pseudo*-tricyclic structure, making it an ideal ligand for complex formation (Scheme 1d). In addition, we hypothesized that incorporation of bulky tertiary alkyl groups at C4 and C5 positions could effectively weaken the intermolecular π-π interaction rendering these complexes solid-state fluorescent dyes. In principle, thiazole **1** could act either as a 1,2- or a 1,3-chelating ligand forming 5-membered or 6-membered chelate, respectively. We report herein a selective synthesis of 5-membered boron difluoro complex **2** and their photophysical properties. Notably, these compounds display fluorescence properties in both solution and solid state with large Stokes shifts ($\Delta\lambda$) and high quantum yields (ϕ_{FL}). Moreover, boron complexes displaying dual fluorescence and room-temperature phosphorescence (RTP) emission properties at both amorphous and crystalline states are documented.

Results and Discussion

Synthesis

The 2-aryl-5-alkylamino-4-alkylaminocarbonylthiazoles **1** were prepared in one step by an yttrium triflate-catalyzed condensation of thiocarboxylic acids **3** with isocyanides **4**.[38] Formation of boron difluoro complexes of **1** was examined using **1a** ($R^1 = Ph$, $R^2 = t$Bu) as a test substrate. After systematic survey of reaction conditions varying the base, the solvent, temperature and the stoichiometry of the reagents (see Supporting Information for details), the optimum conditions consisted of heating to reflux a chloroform solution of **1a** (*c* 0.1 M) in the presence of an excess amount of $BF_3 \cdot Et_2O$ (15.0 equiv.) and diisopropylethylamine (DIPEA, 10.0 equiv.) for 2 h. Under these conditions, the boron complex **2a** was isolated in 84% yield (Scheme 2). Applying the same conditions, a series of boron complexes **2b**–**2u** bearing different substituents on the thiazole ring were prepared in moderate to good yields (Scheme 2). As it is seen, the C2-aromatic substituent bearing a halide (F, Cl, Br, I) was well tolerated affording compounds **2b**–**2e** in good yields. The presence of a strong electron-withdrawing group in the aromatic ring decreased nevertheless significantly the yield of boron complexes (*cf* **2f**, **2g**). Electron-rich arenes were also compatible with the reaction conditions (**2h**–**2j**). The naphthyl, heteroaromatics (furan, thiophene) and extended conjugation system at the C2 position of thiazole were converted to the boron complexes without event (**2k**–**2q**). The boron complexes **2t** and **2u** bearing bulkier alkyl substituents (*tert*-pentyl, 2,4,4-trimethlpentyl) were similarly synthesized. We note that in all these examples, thiazoles **1** acted as a 1,2-N^N chelating ligand affording 5-membered boron complexes **2** exclusively at the expense of the alternative 6-membered boron complexes. The higher basicity of the ring nitrogen vs. the carbonyl group of the amide, the higher acidity of the 4-carboxamide NH vs. the 5-NH might be responsible for the observed selectivity. All new compounds were fully characterized by spectroscopic and elemental analysis. To the best of our knowledge, boron complex with a secondary amide acting as an anionic N donor ligand has not been investigated as potential luminophores.[39]

Photophysical properties

The photophysical properties of these boron complexes **2** were next investigated. The longest absorption maximum, luminescence maximum, Stokes shift and quantum yield in both

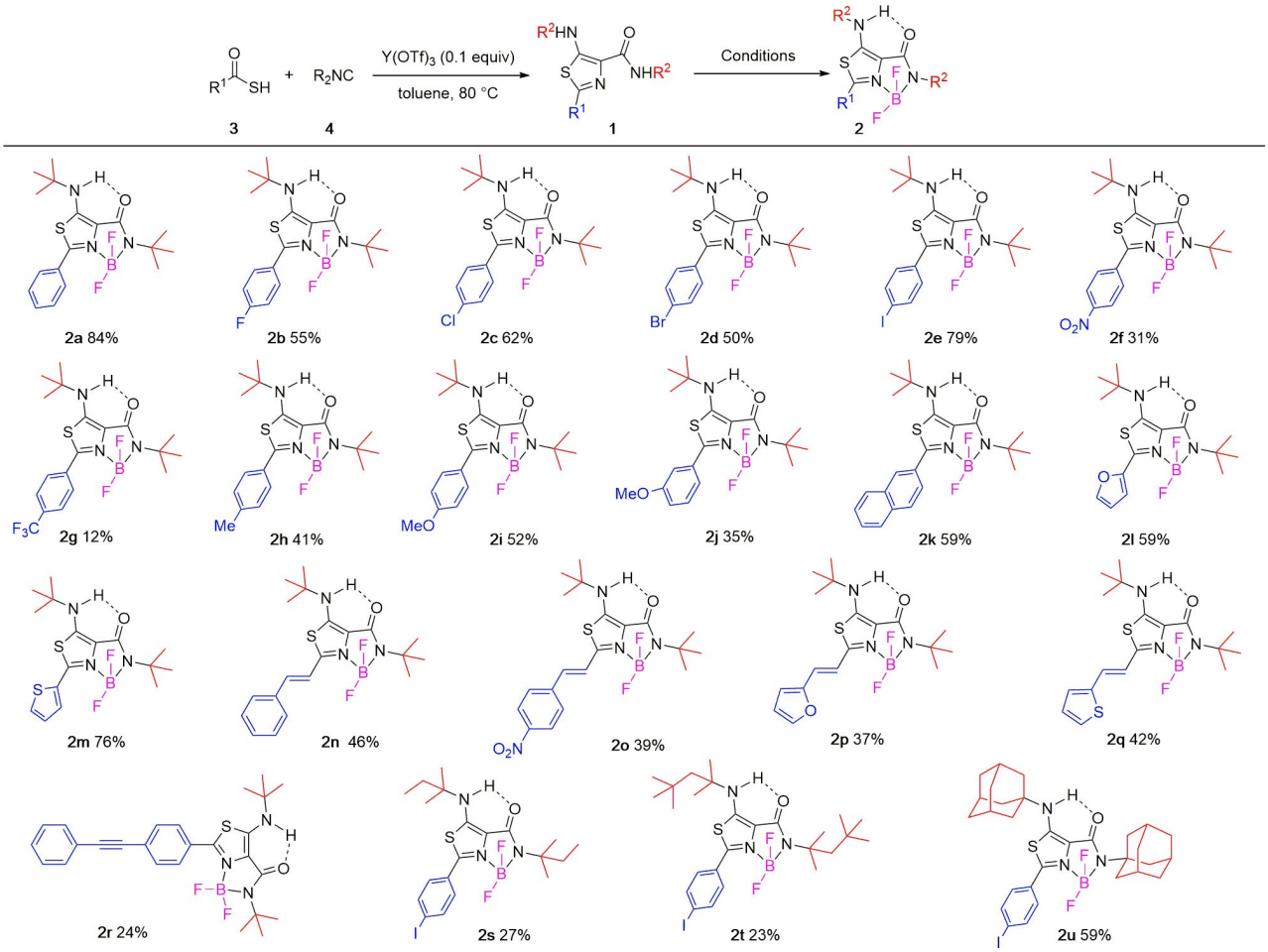

Scheme 2. Synthesis of boron difluoro complex of thiazoles. Conditions: **1** (0.2 mmol), $BF_3 \cdot Et_2O$ (15.0 equiv.), DIPEA (10.0 equiv.), $CHCl_3$ (2.0 mL, *c* 0.1 M), rt then reflux. Yield refers to isolated pure product.

toluene and solid state are summarized in Table 1 (the UV-vis absorption and emission profiles are depicted in Figure S1–S21). These complexes exhibit strong absorption maxima ranging from 381 to 447 nm with high molar absorptivity ($\varepsilon_{max} > 10^4\ M^{-1}cm^{-1}$) and emit at 467 to 526 nm with quantum yield (ϕ_{FL}) up to 71.4%. The Stokes shifts ($\Delta\lambda$) of these compounds are higher than 77 nm (3856 cm^{-1}) which is a desirable feature in order to minimize the reabsorption of emitted photons (Table 1). In comparison with the parent compound **2a**, introduction of strong electron-withdrawing group at the *para* position of the 2-phenyl moiety (**2f**, R = 4-NO_2) results in bathochromic shift of absorption and emission due most probably to the excited state intramolecular charge transfer (ICT) process.[13,14] The DFT calculation reveals that the HOMOs exhibit large electronic coefficients on the 5-membered boron ring, whereas LUMOs are placed on nitrobenzene ring, suggesting ICT from boron to nitrobenzene (Figure S71). Indeed, the emission wavelengths of **2f** and **2o** are solvent-dependent, whereas all other BF_2-complexes are relatively insensitive to solvent polarity (Figure S22–S37). Extending the conjugate system (**2n**–**2r**) gives similar wavelength-tuning effect. In contrast to traditional BODIPY, the dried powder of **2a**–**2r** exhibits bright luminescence under illumination of UV light ($\lambda_{ex} = 365$ nm). We therefore recorded the emission spectra of **2a**–**2r** in solid state, which produced bathochromic shifted fluorescence bands, centering at 479–677 nm, relative to that in solution (Figure 1 and Figure S38–S54). The absolute quantum yields (ϕ_{FL}) of the compounds are in the range of 0.1–34.7% with compound **2h** being the highest.

Interestingly, compound **2e** bearing iodine substituent shows peculiar dual luminescent profiles in solid state. In addition to the normal fluorescence emission at 500 nm ($\phi_{FL} = 1.0\%$, $\tau_{FL} = 135$ ps), a new band indicative of phosphorescence emission at wavelength 662 nm ($\phi_{PL} = 0.2\%$) is observed. The dual phosphorescence and fluorescence could explain the relatively low fluorescence quantum yield (ϕ_{FL}) of **2e** relative to other complexes (with exception of **2p** and **2q**). Phosphorescence mode and lifetime decay measurements confirm that **2e** is an RTP dye with lifetime of 107 μs. Under vacuum and low temperature (77 K), the RTP lifetime increases, as expected, to 160 μs because both conditions in principle could inhibit the non-radiative T1-S0 decay. Notably, **2e** is insensitive to oxygen since identical lifetime is determined under air and vacuum (Table 2). We also recorded the phosphorescence spectra of

Table 1. Photophysical data of boron difluoride complexes **2**.

	toluene λ_{abs} [nm]	ε [$M^{-1}cm^{-1}$]	λ_{em} [nm]	Stokes shift [nm]	ϕ_{FL} [%][a]	solid state λ_{em} [nm]	ϕ_{PL} [%][b]
2a	383	13963	467	84	35.1	483	27.5
2b	381	13881	467	86	49.9	479	26.6
2c	390	15164	472	82	48.9	489	25.4
2d	392	17162	472	80	71.4	488	17.6
2e	394	19180	474	80	11.7	500	1.0
2f	431	17444	513	82	43.7	543	0.1
2g	396	16999	474	78	16.6	483	21.2
2h	383	15135	468	85	64.9	482	34.7
2i	384	17215	471	87	44.7	482	22.6
2j	384	14302	468	84	57.0	475	24.4
2k	398	18638	479	81	17.9	502	18.5
2l	395	17613	473	78	4.7	506	4.9
2m	402	15082	490	88	7.3	525	17.5
2n	417	23260	497	80	11.9	579	7.3
2o	447	26152	526	79	2.8	677	0.1
2p	426	25585	507	81	1.5	643	0.3
2q	414	16052	515	101	0.7	628	1.1
2r	410	25966	487	77	7.1	525	16.9
2s	395	20340	475	80	11.2	485	1.8
2t	399	19190	478	79	27.2	496	1.4
2u	398	18307	480	82	13.3	484	2.1

[a] Quantum yield determined in solution, using quinine sulfate ($\phi = 0.55$ in 1 N H_2SO_4, $\lambda_{ex} = 366$ nm) as reference for dyes ($\lambda_{ex} \leq 395$ nm) or coumarin 343 ($\phi = 0.63$ in ethanol, $\lambda_{ex} = 425$ nm) as reference for dyes ($\lambda_{ex} > 395$ nm). [b] Absolute quantum yield for dyes in solid state.

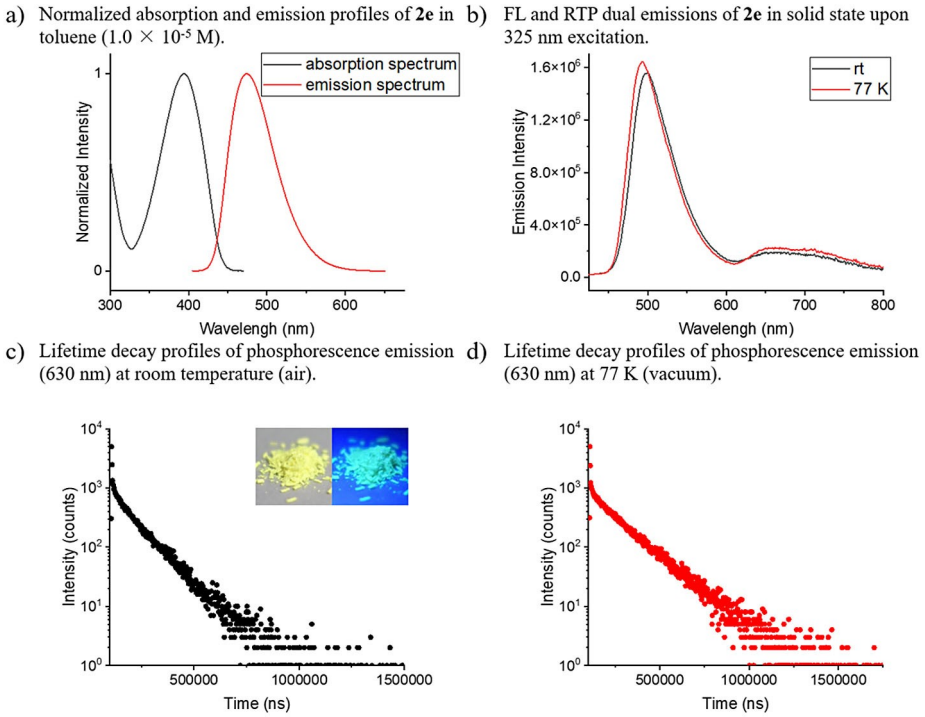

Figure 1. Fluorescence and phosphorescence of compound **2e**.

both the crystalline and amorphous samples of **2e** (Figure 1). To our delight, two samples give similar phosphorescence profiles and lifetime, indicating **2e** is an RTP emitter without requiring rigorous crystal engineering.

The enhanced spin-orbit coupling (SOC) of iodine on the chromophore is known to increase the efficiency of the ISC process, hence the peculiar phosphorescence emission of **2e**. To verify the generality and to investigate the steric effect of substituents, several iodine-containing boron complexes **2s**–**2u** were synthesized. From the data summarized in Table 1 and Figure S19–S21, a toluene solution of **2s**–**2u** shows similar absorption, emission and Stokes shift as that of **2e**. Pleasantly,

Table 2. Emission and phosphorescence property of **2e**, **2s**–**2u** in solid state.

	condition	λ_{FL} [nm]	ϕ_{FL} [%][a]	τ_{FL} [ps]	λ_{PL} [nm]	ϕ_{PL} [%][a]	τ_{PL} [μs]
2e	rt (air)	500	1.0	135	662	0.2	107
	rt (vacuum)	499	–	–	664	–	111
	77 K (vacuum)	493	–	–	662	–	160
2s	rt (air)	485	1.8	217	646	0.3	100
	rt (vacuum)	485	–	–	650	–	103
	77 K (vacuum)	497	–	–	661	–	175
2t	rt (air)	496	1.4	186	661	0.3	165
	rt (vacuum)	497	–	–	664	–	162
	77 K (vacuum)	493	–	–	663	–	203
2u	rt (air)	484	2.1	134	666	0.6	189
	rt (vacuum)	484	–	–	667	–	190
	77 K (vacuum)	485	–	–	672	–	251

[a] Absolute quantum yield for dyes in solid state.

these compounds also exhibit room-temperature phosphorescence, supporting the role of heavy atom (Figure S55-S59). The fluorescence and phosphorescence quantum yields in solid state increase with the enlargement of the alkyl substituents (**2e** < **2s** < **2t** < **2u**). It is interesting to note that increase of substituent size also extends lifetime (τ_{PL}) of the compound with an order of **2e** ≈ **2s** < **2t** < **2u** being observed under three sets of conditions: air, vacuum and low temperature (Table 2).

Crystal structures

To understand the factors responsible for the photophysical properties of thiazole-BF_2 complexes **2** at molecular level, the structure of fluorescence emitters **2a**, **2b**, **2h**, **2k**, **2o** and **2q**, phosphorescence emitters **2e**, **2s**–**2u** were determined by X-ray crystallographic analysis (Tables S4–S13).[40] The planar 5-membered boron complex in all these complexes is coplanar to the thiazole ligand forming therefore a flat bicyclic structure. The nitrogen of amide is sp^2 hybridized, while the boron adopts a distorted tetrahedral geometry. An intramolecular H-bond between the C5-NH and the C4-carboxamide groups (e.g. for **2a**: 2.4 Å) was found in all these complexes, forming a coplanar pseudo-tricyclic structure and restricting the rotation of the C5 aminoalkyl substituent. An additional H-bond between one of the BF_2 groups and the C2-arene C–H (**2a**: 2.3 Å) further reduced the conformational mobility of the complex, essential for the high emission efficiency in the condensed state (Figure 2, 3 and Figure S60–S70). In each structure of **2a**, **2b**, **2h** and **2k**, the bond lengths of B–N thiazole are, as expected, 0.08-0.11 Å longer than those of the B–N amide. The aryl ring and thiazole boron planes tend to twist each other with dihedral angles of 31.06° (**2a**), 30.15° (**2b**), 27.97° (**2h**) and 21.78° (**2k**), respectively. The neighboring complexes adopt a head-to-tail arrangement, interacting each other through C–H…π interaction. The large plane-plane distances are in the range of 3.73–4.13 Å indicating a negligible π-π intermolecular orbital overlap of the fluorophores. The presence of bulky tert-butyl group, protruded out of the plan of boron complex, might effectively disfavor the intermolecular π-π stacking for the steric reason. On the other hand, the intermolecular C–H…π interactions are advantageous to suppress the molecular motion and π-π stacking. The unsymmetric nature of the ligand favors distinct ground and excited states while the packing modes avoid the aggregation-induced quenching. Both structural features contribute to the large Stokes shift and significant solid emission of these complexes. In sharp contrast, complexes **2o** and **2q** bearing extended conjugation moiety show smaller derivation angels between two ends (11.4° and 10.8°), resulting in an improved π electron delocalization, hence a bathochromic shift (solid state: λ_{em} = 677 nm and 628 nm for **2o** and **2q**, respectively). However, the extended conjugation and the co-planarity also enables an intermolecular π-π interaction (< 3.3 Å) which is translated into low quantum yields of these boron complexes both in solution and in solid state.

In the cases of fluorescence and phosphorescence dual emitters **2e**, **2s**–**2u**, despite of the existence of bulky groups or twisting angle between C2 aryl substituents and thiazole boron cores, dimers (plane-to-plane distance < 3.7 Å) are formed through C–H···π or π-π interactions (Figure 5 and Figure S69). Such dimers serve as basic building blocks to form high-level self-assemblies in crystalline state. In the dimers of **2e**, **2s** and **2u**, the aryl moiety and thiazole boron core of two molecules are head-to-tail arrayed. The centroid-centroid distances between neighboring thiazole boron cores are 5.7 Å (**2e**), 5.9 Å (**2s**), and 6.4 Å (**2u**), respectively, in line with the increasing size of *tert*-alkyl substituents. Two units of dimer interact each other through C–I···O halogen bonds ($d_{I\text{-}O}$ = 2.9–3.0 Å), resulting in infinite layer assembly structures. Surprisingly, *tert*-octyl bearing compound **2t** gives different structure. Instead of being twisted, the aryl substituent and thiazole boron core are coplanar. The dimer is formed through head-to-tail intermolecular π-π stackings ($d_{\pi\text{-}\pi}$ = 3.5 Å). Two units of dimer are weakly linked by a secondary π-π stacking ($d_{\pi\text{-}\pi}$ = 3.7 Å) between aryl rings. Besides, the adjacent octyl groups show short contacts through van der Waals interaction. The multiple non-covalent bonds formed in **2t** therefore produce a fishbone-like structure. From these analyses, we postulate that both the presence of iodine and the particular crystal structures contribute to the RTP property of **2e**, **2t**–**2u**. While heavy atom iodine enhances spin-orbit coupling, the self-assembly driven by halogen bonding, π-π and C-H···π interactions significantly reduces the intramolecu-

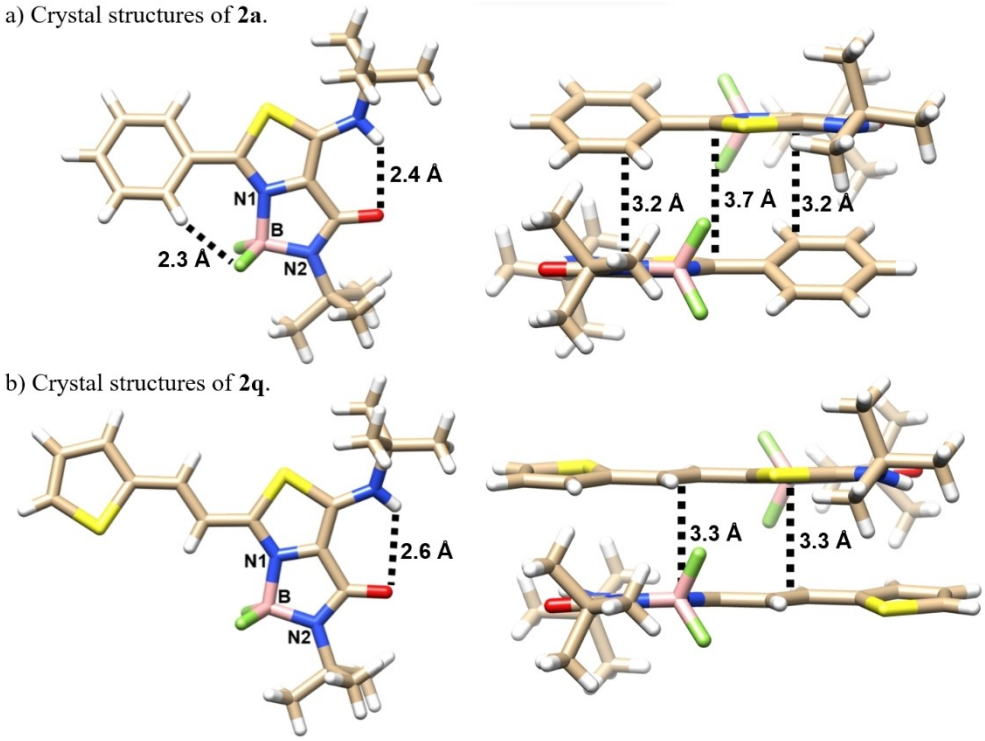

Figure 2. Crystal structures of **2a** (a) and **2q** (b). Selected bond lengths (Å) and angles (°) for **2a**: B–N1 1.6, B–N2 1.5, heterocycle-heterocycle 3.7, C–H···π 3.2, ∠benzene-heterocycle 31.1; Selected bond lengths (Å) and angles (°) for **2q**: B–N1 1.6, B–N2 1.5, π-π 3.3, ∠benzene-heterocycle 10.8.

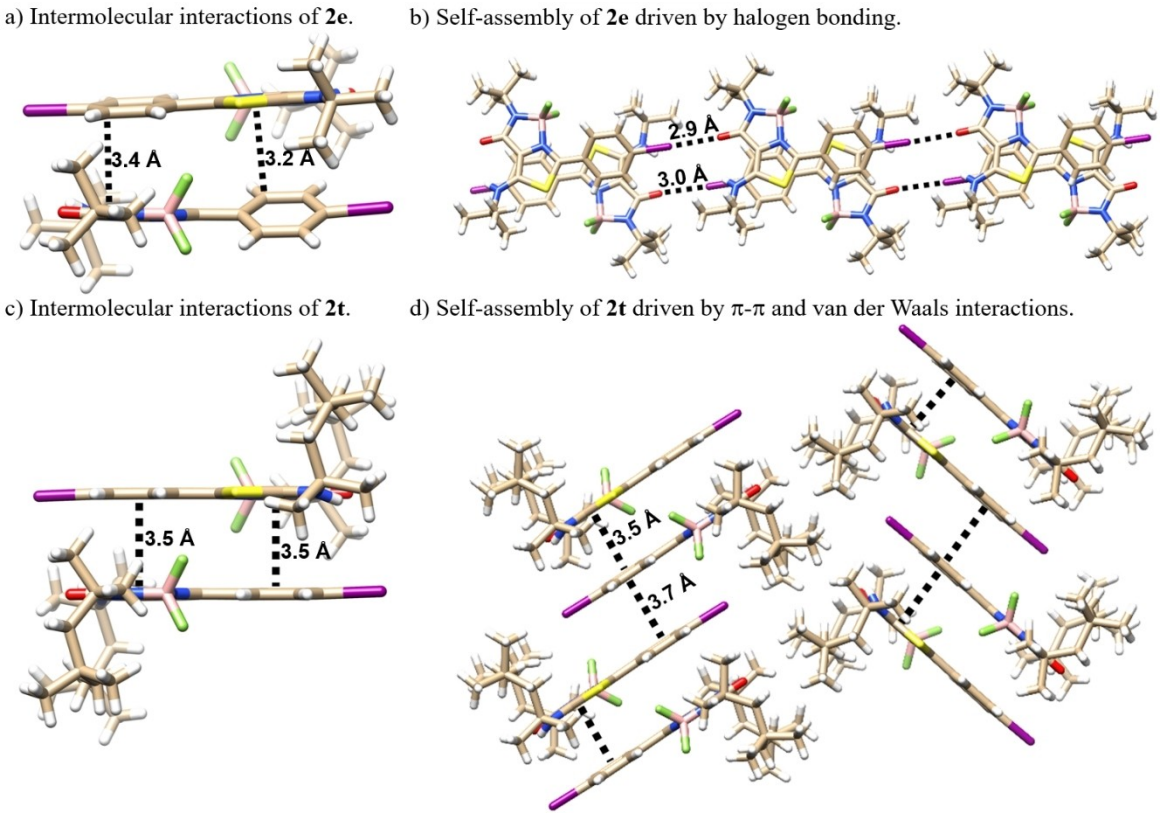

Figure 3. Crystal structures of **2e** and **2t**: intermolecular interactions and self-assembly. Selected bond lengths (Å) and angles (°) for **2e**: B–N1 1.6, B–N2 1.5, I–O 2.9, 3.0, C–H···π 3.2, 3.4, heterocycle-heterocycle 5.7, ∠benzene-heterocycle 28.2, 6.5; Selected bond lengths (Å) and angles (°) for **2t**: B–N1 1.6, B–N2 1.5, π-π 3.5, 3.7, heterocycle-heterocycle 5.4, ∠benzene-heterocycle 1.6.

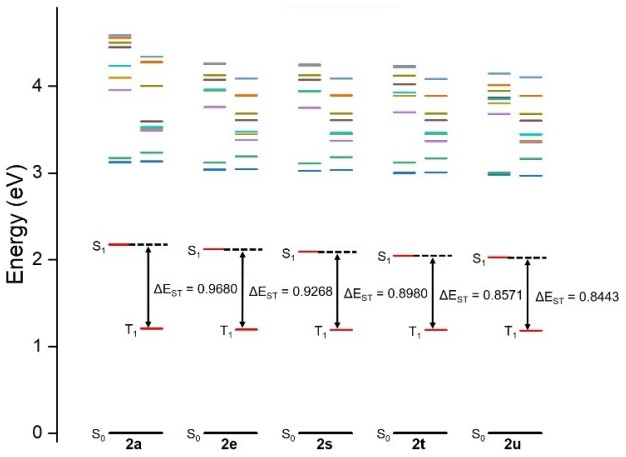

Figure 4. TD-DFT calculated Sn and Tn energies and ΔE_{ST}.

lar rotation freedom of these complexes, hence an emission enhancement. A TD-DFT computations at B3LYP [density functional (6-311G (d, p)] basis set for all atoms except iodine atom, LanL2DZ basis set for iodine atom of theory were performed to calculate the energy gap (ΔE_{ST}) between S1 and T1 states of complexes **2a**, **2e** and **2t**–**2u** (Figure 4). In line with the observed phosphorescence properties of dyes **2e**, **2s**–**2u**, the singlet to triplet energy differences of these complexes (ΔE_{ST} = 0.9268–0.8443 eV) are indeed smaller than **2a** (ΔE_{ST} = 0.9680 eV) which could explain the facile intersystem crossing (ISC) of the dual emitters **2e**, **2s**-**2u**. The continual decrease of ΔE_{ST} from **2e** to **2u** agrees well with the increase of phosphorescence quantum yields and lifetime observed experimentally (Table S14).

Conclusion

We reported in this paper the first examples of boron complex dyes in which a secondary amide served as an anionic ligand of boron. The unsymmetric nature of the ligand structure, negligible π-π intermolecular orbital overlap owing to the twist of C2-substituent from thiazole boron core, and the existence of bulky alkyl groups at C4 and C5 positions of thiazole endow these boron complexes large Stokes shift and significant solid-state emission. Introducing iodine atom into the structure enhanced spin-orbit coupling and intermolecular interaction including halogen bonding, π-π and C–H···π interactions facilitate triplet state emission. The RTP property could be fine-tuned by changing the size of the bulky alkyl substituents. This work demonstrates that amorphous small organic molecules with FL and RTP dual emission properties can be designed through tailoring the ligand structure of boron complex.

Experimental Section

Synthesis of thiazole: A suspension of thiocarboxylic acid **3** (2.50 mmol), isocyanide **4** (12.50 mmol, 5.0 equiv.) and $Y(OTf)_3$ (0.25 mmol, 0.10 equiv.) in toluene (50 mL, *c* 0.05 M) was heated to 80 °C under argon atmosphere. Upon completion, the mixture was quenched with saturated aqueous $NaHCO_3$ and extracted with ethyl acetate. The combined organic layers were washed with brine, dried over Na_2SO_4 and concentrated under reduced pressure. The crude mixture was then purified by flash column chromatography (silica gel) to give the desired carboxamidothiazole **1**.

Synthesis of thiazole-boron complex: A solution of carboxamidothiazole **1** (0.20 mmol) and DIPEA (2.0 mmol, 10.0 equiv.) in $CHCl_3$ (2.0 mL, *c* 0.10 M), was stirred under argon atmosphere at room temperature for 15 min. $BF_3 \cdot Et_2O$ (3.0 mmol, 15.0 equiv.) was added and the resulting mixture was stirred at room temperature for 15 min. The solution was heated to reflux until the complete consumption of the starting materials. The reaction was quenched with H_2O and the aqueous layer was extracted with dichloromethane. The combined organic layers were dried over Na_2SO_4 and concentrated under reduced pressure. The residue was purified by flash column chromatography (silica gel) to give the desired carboxamidothiazole BF_2-complex **2**.

Photophysical measurements: For measurement in solution, a stock solution was prepared by dissolving the thiazole BF_2-complex **2** in toluene (8.0×10^{-5} M). The stock solution was diluted to 2.0×10^{-5} for absorption, and 1.0×10^{-5} M for excitation and emission spectra recording, respectively. The spectra were recorded at room temperature. Transient phosphorescence decay profiles of thiazole BF_2-complex **2** for solid state were measured on a FLS-1000 instrument equipped with a liquid nitrogen cryostat, data at room temperature and low temperature under air or vacuum (~10^{-6} mbar) were recorded. Transient fluorescence decay profiles were recorded on a Coherent Astrella-Opera Solo femto second ultrafast spectroscopy. Absolute quantum yields for solid were measured with an integrating sphere at room temperature under air.

Crystallographic analysis: The single crystal of thiazole BF_2-complex **2a** was cultivated by slow evaporation of petroleum ether/ethyl acetate/CH_2Cl_2 at rt. **2b** was cultivated by recrystallization in ethyl ether at reflux temperature to rt. **2e**, **2h**, **2k**, **2o**, **2q**, **2s**, **2t** and **2u** was cultivated by slow evaporation of *n*-hexane/CH_2Cl_2 at rt. X-ray intensity data were collected on a XtaLAB Synergy R, HyPix diffractometer for the structures using CuKα (λ = 1.54184 Å) at setting temperatures. The intensity data were collected by the omega scans techniques, scaled, and reduced with CrysAlisPro. The correction of the collected intensities for absorption was done using the CrysAlisPro program. The structures were solved by direct methods using SHELXT and refined using full-matrix least-squares methods in ShelXL. All non-hydrogen atoms were refined anisotropically depending on the occurrence of disorder in the structures. All hydrogen atoms were placed geometrically and with a riding model for their isotropic temperature factors.

Acknowledgements

We thank the National Natural Science Foundation of China (91956126, 22171160), EPFL (Switzerland) and Swiss National Science Foundation (SNSF 200020-169077) for financial support. Open Access funding provided by École Polytechnique Fédérale de Lausanne.

Conflict of Interest

The authors declare no conflict of interest.

Data Availability Statement

The data that support the findings of this study are available in the supplementary material of this article.

Keywords: boron complex · dyes · halogen bonding · room-temperature phosphorescence · solid state emission

[1] A. Loudet, K. Burgess, *Chem. Rev.* **2007**, *107*, 4891–4932.
[2] D. Frath, J. Massue, G. Ulrich, R. Ziessel, *Angew. Chem. Int. Ed.* **2014**, *53*, 2290–2310; *Angew. Chem.* **2014**,*126*, 2322–2342.
[3] T. Kowada, H. Maeda, K. Kikuchi, *Chem. Soc. Rev.* **2015**, *44*, 4953–4972.
[4] Z. Shi, X. Han, W. Hu, H. Bai, B. Peng, L. Ji, Q. Fan, L. Li, W. Huang, *Chem. Soc. Rev.* **2020**, *49*, 7533–7567.
[5] A. Bessette, G. S. Hanan, *Chem. Soc. Rev.* **2014**, *43*, 3342–3405.
[6] B. M. Squeo, L. Ganzer, T. Virgili, M. Pasini, *Molecules* **2021**, *26*, 153.
[7] N. Boens, V. Leen, W. Dehaen, *Chem. Soc. Rev.* **2012**, *41*, 1130–1172.
[8] H. Lu, J. Mack, Y. Yang, Z. Shen, *Chem. Soc. Rev.* **2014**, *43*, 4778–4832.
[9] J. F. Araneda, W. E. Piers, B. Heyne, M. Parvez, R. McDonald, *Angew. Chem. Int. Ed.* **2011**, *50*, 12214–12217; *Angew. Chem.* **2011**,*123*,12422–12425.
[10] Y. Ren, X. Liu, W. Gao, H. Xia, L. Ye, Y. Mu, *Eur. J. Inorg. Chem.* **2007**, 1808–1814.
[11] H.-X. Luo, Y. Niu, X. Jin, X.-P. Cao, X. Yao, X.-S. Ye, *Org. Biomol. Chem.* **2016**, *14*, 4185–4188.
[12] H. Liu, H. Lu, J. Xu, Z. Liu, Z. Li, J. Mack, Z. Shen, *Chem. Commun.* **2014**, *50*, 1074–1076.
[13] C. Maeda, T. Todaka, T. Ema, *Org. Lett.* **2015**, *17*, 3090–3093.
[14] M. Más-Montoya, M. F. Montenegro, A. E. Ferao, A. Tárraga, J. N. Rodríguez-López, *Org. Lett.* **2020**, *22*, 3356–3360.
[15] J.-S. Ni, H. Liu, J. Liu, M. Jiang, Z. Zhao, Y. Chen, R. T. K. Kwok, J. W. Y. Lam, Q. Peng, B. Z. Tang, *Mater. Chem. Front.* **2018**, *2*, 1498–1507.
[16] Y.-Y. Wu, Y. Chen, G.-Z. Gou, W.-H. Mu, X.-J. Lv, M.-L. Du, W.-F. Fu, *Org. Lett.* **2012**, *14*, 5226–5229.
[17] R. Yoshii, K. Suenaga, K. Tanaka, Y. Chujo, *Chem. Eur. J.* **2015**, *21*, 7231–7237.
[18] K. Benelhadj, J. Massue, P. Retailleau, G. Ulrich, R. Ziessel, *Org. Lett.* **2013**, *15*, 2918–2921.
[19] D. Zhao, G. Li, D. Wu, X. Qin, P. Neuhaus, Y. Cheng, S. Yang, Z. Lu, X. Pu, C. Long, J. You, *Angew. Chem. Int. Ed.* **2013**, *52*, 13676–13680; *Angew. Chem.* **2013**, *125*, 13921–13925.
[20] Q. Hao, S. Yu, S. Li, J. Chen, Y. Zeng, T. Yu, G. Yang, Y. Li, *J. Org. Chem.* **2014**, *79*, 459–464.
[21] Y. Yang, X. Su, C. N. Carroll, I. Aprahamian, *Chem. Sci.* **2012**, *3*, 610–613.
[22] W. Li, W. Lin, J. Wang, X. Guan, *Org. Lett.* **2013**, *15*, 1768–1771.
[23] T. Nakano, A. Sumida, K. Naka, *ChemistrySelect* **2021**, *6*, 1168–1173.
[24] X. Wang, Q. Liu, F. Qi, L. Li, H.-D. Yu, Z. Liu, W. Huang, *Dalton Trans.* **2016**, *45*, 17274–17280.
[25] H. Liu, H. Lu, Z. Zhou, S. Shimizu, Z. Li, N. Kobayashi, Z. Shen, *Chem. Commun.* **2015**, *51*, 1713–1716.
[26] C. Cheng, N. Gao, C. Yu, Z. Wang, J. Wang, E. Hao, Y. Wei, X. Mu, Y. Tian, C. Ran, L. Jiao, *Org. Lett.* **2015**, *17*, 278–281.
[27] K. I. Lugovik, A. K. Eltyshev, P. O. Suntsova, P. A. Slepukhin, E. Benassi, N. P. Belskaya, *Chem. Asian J.* **2018**, *13*, 311–324.
[28] B. Lee, B. G. Park, W. Cho, H. Y. Lee, A. Olasz, C.-H. Chen, S. B. Park, D. Lee, *Chem. Eur. J.* **2016**, *22*, 17321–17328.
[29] M.-C. Chang, A. Chantzis, D. Jacquemin, E. Otten, *Dalton Trans.* **2016**, *45*, 9477–9484.
[30] D. Cappello, D. A. B. Therien, V. N. Staroverov, F. Lagugné-Labarthet, J. B. Gilroy, *Chem. Eur. J.* **2019**, *25*, 5994–6006.
[31] S. Hapuarachchige, G. Montaño, C. Ramesh, D. Rodriguez, L. H. Henson, C. C. Williams, S. Kadavakkollu, D. L. Johnson, C. B. Shuster, J. B. Arterburn, *J. Am. Chem. Soc.* **2011**, *133*, 6780–6790.
[32] J. Zhao, K. Xu, W. Yang, Z. Wang, F. Zhong, *Chem. Soc. Rev.* **2015**, *44*, 8904–8939.
[33] X.-F. Wang, H. Xiao, P.-Z. Chen, Q.-Z. Yang, B. Chen, C.-H. Tung, Y.-Z. Chen, L.-Z. Wu, *J. Am. Chem. Soc.* **2019**, *141*, 5045–5050.
[34] T. Zhang, X. Ma, H. Wu, L. Zhu, Y. Zhao, H. Tian, *Angew. Chem. Int. Ed.* **2020**, *59*, 11206–11216; *Angew. Chem.* **2020**, *132*, 11302–11312.
[35] T. Zhang, X. Ma, H. Tian, *Chem. Sci.* **2020**, *11*, 482–487.
[36] D. Li, F. Lu, J. Wang, W. Hu, X.-M. Cao, X. Ma, H. Tian, *J. Am. Chem. Soc.* **2018**, *140*, 1916–1923.
[37] H. Wu, C. Hang, X. Li, L. Yin, M. Zhu, J. Zhang, Y. Zhou, H. Ågren, Q. Zhang, L. Zhu, *Chem. Commun.* **2017**, *53*, 2661–2664.
[38] S. Tong, S. Zhao, Q. He, Q. Wang, M.-X. Wang, J. Zhu, *Angew. Chem. Int. Ed.* **2017**, *56*, 6599–6603; *Angew. Chem.* **2017**, *129*, 6699–6703.
[39] Six-membered borates using secondary amide as an anionic O donor is known, see Ref. [16].
[40] Deposition Numbers 993648 (for **2a**), 2173871 (for **2b**), 2173872 (for **2e**), 2173873 (for **2h**), 2173874 (for **2k**), 2173875 (for **2o**), 2173876 (for **2q**), 2173877 (for **2s**), 2173878 (for **2t**), 2173879 (for **2u**) contain the supplementary crystallographic data for this paper. These data are provided free of charge by the joint Cambridge Crystallographic Data Centre and Fachinformationszentrum Karlsruhe Access Structures service.

Manuscript received: August 11, 2022
Accepted manuscript online: August 22, 2022
Version of record online: September 19, 2022